Volume 16, Number 5, 2023. pp. 551-561

Jordan Journal of Physics

ARTICLE

Program for Calculating the Axial Magnetic Field Distribution of Magnetic Lenses Using Finite Element Method

Abdullah I. M. Alabdullah[a], **Ezaldeen M. A. Alkattan**[b] and **R.Y. J. Al-Salih**[c]

[a] *Department of Physics, College of Sciences, Mosul University, Mosul, Iraq.*

[b] *the General Directorate for Education in Nineveh, Iraq.*

[c] *Department of Physics, College of Sciences, Tikrit University, Tikrit, Iraq.*

Doi: https://doi.org/10.47011/16.5.6

Received on: 15/01/2022; *Accepted on: 12/06/2022*

Abstract: Introducing FEM-CMFD (Finite Element Method for Calculating Magnetic Field Distribution), a new program designed for calculating the magnetic field distribution for axially symmetric complex magnetic systems, such as magnetic lenses. The program operates by reading user-inputted magnetic system data presented in a two-dimensional graph. Utilizing the finite element method, it calculates the axial magnetic field distribution for various coil excitations accommodating up to approximately 10 000 intersection nodes.

Keywords: Electron magnetic lens, Finite element method, Magnetic field distribution.

Introduction

The history of electron microscopy started with the development of electron optics. In 1926, Busch excogitated the charged particle trajectories in axially symmetric magnetic and electric fields in 1926. He laid the foundation of geometrical electron optics, and he proved that such fields could act as particle lenses. Around the same time, de Broglie presented the principle of electron waves [1]. A wavelength in addition to a frequency was associated scientifically with the charged particles, and this point presented the beginning of electron optics. These breakthroughs paved the way for the realization of an electron microscope [2]. The electron lens, a crucial component of electron microscopes, is also a fundamental part of various electro-optical devices [3]. There are three primary types of lenses: electrostatic lenses, permanent magnetic lenses, and electromagnetic lenses. Among these, electromagnetic lenses are commonly preferred due to factors such as ease of manufacturing, simplicity of use, high precision results, and cost-effectiveness. It should be mentioned that various abuses in electron lenses can occur during manufacturing, such as "aberrations" caused by the lens structure's failure to focus all the charged particles emitted from any point on the "object's plane" into one point on the "image Gaussian plane". Thus, the resulting image may be either "askew" or "obscured". Therefore, there is an urgent need to control the charged particles' behavior by using an equivalent optical tool [4]. When this accurate tool is unavailable, it becomes necessary to create many lenses until achieving the desired properties of the designed lens through trial and error, involving significant efforts and costs. Various simulators, software program collections, and mathematical models, in conjunction with Computer-Aided Design (CAD) tools, are employed for this purpose.

The CAD of an optical system usually proceeds via three steps. The first step is to compute the magnetic or electric fields from the initial or boundary conditions, while the second step is to compute the representative electron

Corresponding Author: R.Y. J. Al-Salih **Email**: r.y.jasim@tu.edu.iq

trajectories from calculations of the magnetic fields. The third step involves calculating both aberration values and imaging properties from the computed trajectories [5]. CAD tools employed for both electrostatic and electromagnetic lenses are software application packages developed to help users in designing symmetric and asymmetric lenses, including "single, double, and multipolepiece lenses" used in electron microscopy (EM) within the field of electron optics (EO). CAD proves to be a powerful tool for designers of electron optical systems, allowing them to test a lot of different designs without the need for physical manufacturing [6].

Literature Review

In the literature, various software packages and simulators have been employed for electrostatic lens simulations. Some notable examples include SPOC software [7], G-Optk simulation software [8], EOD program [9], CPO programs [10], Focus software [11], SIMION software [12,13], EOS Simulator [14], MEBS software [15], Omni Trak software [16]. These tools offer users the flexibility to choose an appropriate mathematical model, either by selecting an equipped electrostatic field model or by choosing from available models within the software, such as the Glaser model [17], Grivet Lenz model [18], Gaussian model [18], Spherical model [19], Exponential model [19], and others. Electrostatic lens programs play a vital role in all designing processes. Utilizing confirmed software tools not only ensures improved output for designers but also contributes to a significant reduction in time, a crucial factor in electrostatic lens simulation. This efficiency leads to reduced effort and costs, further emphasizing the benefits of evolutionary software tools in the field [20].

In 2013, Hasan *et al*. wrote a new software for electromagnetic lenses known as "CADTEL". This software is designed to operate on various PC systems, offering the capability to obtain and integrate two distinct procedures [21]. Additionally, in 2016, simulators referred to as "FWHMs" were employed to estimate multi-wavelengths and polarization-insensitive lenses based on the dielectric met surfaces with the met particles [22].

Optimization through analysis has garnered significant attention since the middle of the previous century. Various concepts have been explored in the realm analysis methodology, including the impact of pole piece saturation on the focal characteristics of the target lens [23] and the influence of axial magnetic field distribution on the asymmetry of the objective lens in high-voltage electron microscopy [24]. The first methodology is called the "examination/analysis methodology" and depends on the experimentation that includes three categories known as "H1 programs" for magnetic scalar potential together with using and understanding of the Laplace conditions [25] and "H2 and H3 programs" for magnetic vector potential, addressing the conditions of Poisson [26]. The second methodology is the "H4 programs" for the "union/synthesis method". The researchers usually use the Visual Basic language to write their proposed programs. In 2018, Kadhem *et al.* used the finite element method with the aid of Munro programs to study asymmetrical magnetic lenses in conjunction with the Electron Optical Design (EOD) software [27]. Similarly, in 2018, Van Tilborg *et al.* employed MHD simulations for experiments, demonstrating the effectiveness of a discharge capillary in dynamic plasma lenses for concentrating 100 MeV LPA beams [28]. In 2109, Shiltsev *et al.* reworked the FMA and DA plots for illustrative instances of 7 TeV protons flux without affecting the concentrating optics displays in HL- LHC optics, Version 1.0 [29].

In 2019, Alabdullah *et al.* introduced a new development design that they called Focal Length Measurement (FLM), which employs analytical measurement procedures to assess the properties of electrostatic lenses. The FLM method was specifically tested by calculating the focal lengths of electrostatic immersion lenses. The FLM method enables the users and the researchers to obtain the data for different applications. Besides, the FLM method can be used for calculating the focal lengths of new designs of the immersion electrostatic lenses for electron microscopes, as evidenced by high-accuracy results obtained from electron microscope experiments. Additionally, most of the categories of electrostatic lenses could be analyzed with some simple modifications of the FLM method [30]. In the context of this work, a modern program has been written for fast and accurate analytical calculations. This program is designed to calculate the axial magnetic field distribution of magnetic lenses using the finite

element method. This kind of program can be also successfully applied to electron gun designs and any new design of electron magnetic lenses [31].

The Finite Element Method (FEM)

The Finite Element Method (FEM) is a numerical technique employed to solve problems related to boundary value potentials. It was introduced by Munro in 1971 to find solutions to magnetic field problems in electron lenses in electron optics [32]. In this method, the lens is divided into a mesh consisting of numerous small quadrilaterals known as finite elements, facilitating analysis. Each quadrilateral is further subdivided into double triangular finite elements, and this sub-division is accomplished in two separate ways [33].

The triangular shape is the most elementary type of element, leading to the widespread use of triangular mesh grids rather than rectangular meshes. This allows the evaluation of the potential value for each mesh point. The potential value is assumed to change linearly over each triangular finite element. Consequently, the potential equation for a symmetric magnetic electron lens can be expressed as:

$$F = \iint \frac{1}{2} \cdot \mu \cdot \left[\left(\frac{\partial V}{\partial z}\right)^2 + \left(\frac{\partial V}{\partial r}\right)^2\right] \cdot 2 \cdot \pi \cdot r \cdot dz \cdot dr \quad (1)$$

where μ is the permeability at any point, and V is the scalar potential.

Equation (1) must now be minimized at each mesh point numerically. The contribution of Δf from each single finite element according to the equation (1) becomes:

$$\Delta f = \frac{\pi \cdot \mu \cdot r_\circ}{4a}\left[\left(\sum_{i=1}^{3} b_i \cdot V_i\right)^2 + \left(\sum_{i=1}^{3} c_i \cdot V_i\right)^2\right] \quad (2)$$

where $r_\circ$ is the value of r at a center point (centroid) of element, a is the area of the element, $b_i = r_j - r_k$, $c_i = z_k - z_j$, and V_i is the scalar potential at each triangular mesh point. From this last relation, it is easy to set up the nodal equation for each mesh point. The set of all the nodal equations obtained can be solved by a matrix method to get the vector potential value for each nodal point.

Mesh Generation

To employ the FEM for magnetic electron lenses, the first step involves specifying the boundaries and positions of magnetic materials and coils using a coarse mesh. The identification of the lens geometry doesn't rely on the fine mesh lines generated between coarse mesh lines in both radial and axial directions [35].

The operator responsible for generating the fine mesh needs to balance memory requirements for the entire program and the computation time to keep them manageable. This is achieved by using a variable mesh size with a concentrated distribution of mesh points around critical areas of the lens, such as the polepiece, and a sparse mesh in other parts of the magnetic lens.

A well-suited mesh distribution ensures accurate calculations of the field distribution, which can be verified by computing the degree of coincidence between the field integral and the designed lens excitation. Therefore, the accuracy of the finite element calculations strongly depends on the compatible choice of meshes, which is largely influenced by the experience of the operator [36].

Evaluating the Percentage Errors in Finite Elements Calculation

The numerical method is used to determine the accuracy of computing the axial flux density. From Ampere's law for a coil with N turns carrying current (I), it is well known that [37]:

$$\oint H \cdot dl = NI \quad (3)$$

where H is the magnetic field, that it is related to the flux density B, which is given by the relation:

$$B = \mu_\circ \cdot \mu_r \cdot H \quad (4)$$

where ($\mu_\circ \cdot \mu_r$) is the permeability of material.

In a finite element program, the flux density is supposed to be zero at the boundaries of the lens. Thus, by combining Eqs. (3) and (4) the following formula can be obtained:

$$\int_{z_1}^{z_2} B \cdot dz = \mu_\circ \cdot \mu_r \cdot NI \quad (5)$$

where z_1 and z_2 are the coordinates of the start and end of the axis, respectively. Therefore, the numerical integration over the length of the optical axis produces a means of calculating the output excitation $(NI)_{out}$. This output excitation value will be compared with the input excitation

$(NI)_{in}$, which is identified in the input data, and then the percentage error of finite element calculation can be calculated from the following equation:

$$Error\% = \left|100 \cdot \left(1 - \frac{(NI)_{out}}{(NI)_{in}}\right)\right| \quad (6)$$

Analysis of the Magnetic Lenses

The use of the computer in the design of magnetic electron lenses and understanding their properties is discussed here, the process commonly referred to as computer-aided design (CAD) of an electron optical system. This process typically involves three steps. The first step is calculating the electric or magnetic field based on initial boundary conditions. The second step is the evaluation of representative electron trajectories based on the calculated magnetic fields. The third step is the calculation of both image properties and aberration values derived from the computed trajectories [5].

Magnetic Field Calculations

In the first step, which involves finding the distribution of the electromagnetic potential or field for a specific geometry of coil, magnetic material, and insulator, three numerical methods are commonly employed to solve the boundary problems in electron optics. These methods are the boundary element method (BEM), the finite difference method (FDM), and the finite element method (FEM) [38-40]. BEM is suitable for solving linear problems that do not require partitioning of the entire space. It is applied to calculate the field of electron guns in electron microscopy. This method focuses on applying the potential only on the material boundaries. FDM is relatively easy to program, but it can be challenging to handle complex designs of electron lenses, especially in the presence of magnetic material saturation. Therefore, it is typically used for designs involving electrostatic lenses. FEM is highly favorable in electron optics as it can handle complex lens geometries effectively. It is particularly useful for addressing the saturation of magnetic materials. The versatility of FEM makes it a preferred choice for various electron optics applications [41].

The axial flux density distribution $B(z)$ is needed for estimating the optical properties. In free space regions, it is well known that $B = \mu_\circ H$ and $H = \nabla\Phi_m$. From these relation, it can be found that [42]:

$$B(z) = \mu_\circ \Phi'_m(z) \quad (7)$$

where $\Phi'_m(z)$ is the derivative of the magnetic potential $\Phi_m(z)$ on the optical axis with respect to z. Then, the axial flux density distribution $B(z)$ can be calculated by numerical differentiation of $\Phi_m(z)$ using the cubic spline curve. Once calculated, the axial flux density distribution B(z) can be graphically represented.

The paraxial rays $r(z)$ can also be calculated by solving the paraxial ray equation for the magnetic lens using the following relation:

$$r''(z) + \frac{e}{8mV} B^2(z) r(z) = 0 \quad (8)$$

where (e/m) is the (charge/mass) ratio of the particle (absolute value) and V is the beam voltage. Equation (8) can be solved numerically using a fourth-order Runge-Kutta formula. After evaluating the axial flux density $B(z)$, its axial derivative $B'(z)$ can be also calculated by numerical differentiation using a cubic spline curve. The aberration coefficients can be calculated by computing suitable integrals. For example, the formulae for calculating the spherical aberration coefficient C_s and the chromatic aberration coefficient C_c, related to the image plane z_i are:

$$C_s = \frac{e}{128mV} \frac{1}{r'^4(z_i)} \int_{z_\circ}^{z_i} \left(\frac{3e}{mV} B^2 r^2 + 8B'^2 r^2 - 8B^2 r'^2 \right) r^2 dz \quad (9)$$

$$C_i = \frac{e}{8mV} \frac{1}{r'^2(z_i)} \int_{l_\circ}^{l_i} B^2 r^2 dz \quad (10)$$

where $r(z)$ is the paraxial ray that begins from the axis at the object plane z_o and crosses the axis again at the image plane z_i and the integrals are computed from z_0 to z_i. The integrals can be also calculated numerically using Simpson's rule. Similarly, this formulae can also be used to calculate the primary field aberrations (coma, astigmatism, field curvature, distortion, and the chromatic field aberrations). The comprehensive aberration formulas are extensively documented in existing literature [43-45].

Now, it is necessary to calculate the potential distributions at all the mesh points of a given design. Since the analysis region contains coil windings, the magnetic vector potential (A) should be used as well. It is defined in such a way that the magnetic flux density (B) is given by ($B = \nabla \times A$). The distribution of (A) can be calculated by minimizing the following variational functional:

$$F = \iiint \left(\frac{1}{2\mu} (\nabla \times A) \cdot (\nabla \times A) - J \cdot A \right) dV \quad (11)$$

where J is the current density (a specific value inside the coil windings and zero value outside the coil windings) and dV represents a small element of volume. In cylindrical coordinates (z,r,θ), the vector potential (A) has three known components (A_z, A_r, A_θ). When the lens is of a rotationally symmetric type, however, the field can be indicated by a vector potential that has only a θ component (A_θ), and then, in terms of (A_θ) Eq. (11) can be written as

$$F = \iint \left\{ \frac{1}{2\mu} \left[\left(\frac{\partial A_\theta}{\partial z} \right)^2 + \left(\frac{\partial A_\theta}{\partial z} + \frac{A_\theta}{r} \right)^2 \right] - J_\theta A_\theta \right\} 2\pi r \, dz \, dr \quad (12)$$

After computing the vector potential (A_θ) at each mesh point, the magnetic flux distribution can be calculated by plotting the contours of the value ($\Psi = 2\pi r A_\theta$). Physically, the quantity Ψ (z,r) at any point (z, r) will represent the total magnetic flux (in webers) enclosed within a coaxial circle of radius r centered at the point under consideration.

The components of the flux density (B_z,B_r), and the total flux density (B) at any given point within the lens can be calculated using the formula listed below:

$$B_z = \frac{\partial A_\theta}{\partial r} + \frac{A_\theta}{r}, B_r = -\frac{\partial A_\theta}{\partial z}, B = \sqrt{B_z^2 + B_r^2} \quad (13)$$

The partial derivatives $(\frac{\partial A_\theta}{\partial z})$ and $(\frac{\partial A_\theta}{\partial r})$ in Eq. (13) can be obtained by numerical differentiation of the quantities of (A_θ) at the mesh point. After calculating the values of (B) at each mesh point, the contours of (B) can also be plotted. These quantities of (B) are very useful for designing magnetic lenses, enabling the prevention of saturation effects in the magnetic material. The saturation effect of axial magnetic fields is shown in Fig. 6 for NI = 20 -100 kA-t. This figure has been generated using the newly developed program referred to as FEM-CMFD. This data is important for researchers, aiding in the avoidance of undesirable situations related to saturation effects.

The axial flux density distribution $B(z)$ is needed for calculating the optical properties. In terms of $A_\theta(z,r)$ this is given mathematically from Eq. (13) by:

$$B(z) = \lim_{r \to 0} \left(\frac{\partial A_\theta}{\partial r} + \frac{A_\theta}{r} \right) = \lim_{r \to 0} \left(\frac{2A_\theta}{r} \right) \quad (14)$$

This value can be computed numerically by taking the quantities of (A_θ) at the first two off-axis mesh points in the radial direction. By signifying these values (A_1 and A_2) and their off-axis distance by r_1 and r_2, respectively, the axial flux density can be given by:

$$B(z) = \frac{r_1^2 A_1 - r_1^3 A_2}{r_1 r_2 (r_2^2 - r_1^2)} \quad (15)$$

Determination of Magnetic Field:

This paper introduces a new program, denoted FEM-CMFD, designed for calculating the axial magnetic field distribution in axially rotating magnetic lenses of any type. The program is based on the boundary conditions of the finite element method (FEM) and utilizes an input method format and computation formulation derived from the set of Munro programs (M12 and M13) [46]. Developed for ease of use, the FEM-CMFD program streamlines the input data preparation and output data presentation. Both input and output data are simplified and can be easily created or edited using Microsoft Excel or any text editor. The program itself has been coded using Microsoft Visual Studio.

The program interface is illustrated in Fig. 1. This interface allows users to open previously created data or generate an Excel sheet for input data based on the selected numbers of vertical and horizontal course meshes, as well as the number of sections on the magnetic lens. Upon opening the data file (via the "Open Input Data" button), the program automatically calculates and displays results in the "Messages" section. In case of errors in the input data file, relevant messages appear in this section, providing information about the type of error and terminating the calculation process.

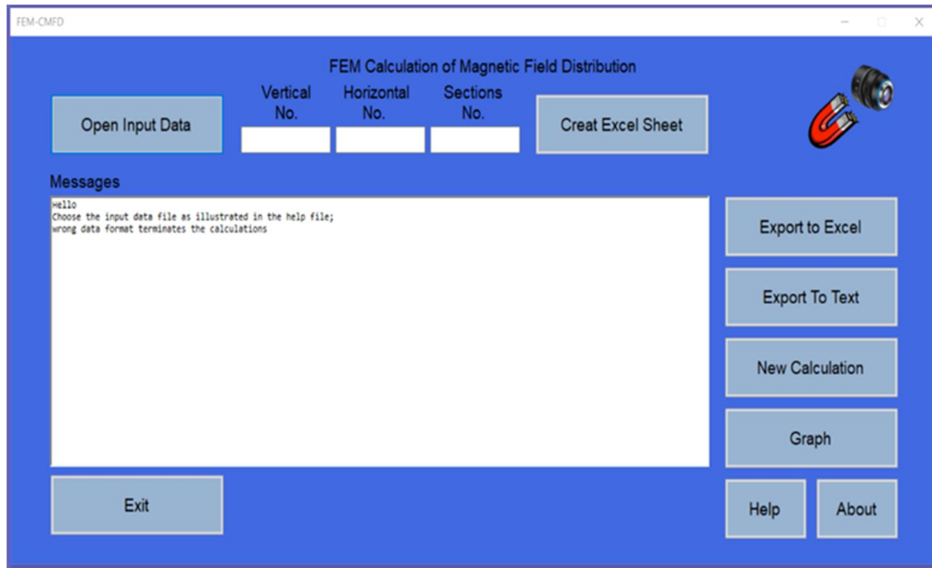

FIG. 1. interface window of FEM-CMFD program.

Fig. 2 shows a sample data preparation for a typical lens. The dataset is identical to the method introduced by Munro [46]. The data in this figure have been structured in Microsoft Excel for simplicity, replacing the older DOS editors. This ensures compatibility with any program that operates under DOS or Windows, offering easy editing. The figure provides comprehensive information on FEM data preparation for magnetic lenses. Additionally, a help file is available and can be accessed via the Help button.

Discribtion Line	Test 4										
basic information	11	9	14	0	0	1	0	0	0	0	
Vertical mesh distribution	1	2	5	7	27	42	52	62	72	82	97
Horizantal mesh distribution	1	2	5	7	25	35	55	65	71		
Horizantal Coordinate	-110	-100	-80	-60	-45	-30	-10	-2	7	20	50
	-110	-100	-80	-60	-45	-30	-10	-2	7	20	50
	-110	-100	-80	-60	-45	-30	-10	-2	7	20	50
	-110	-100	-80	-60	-45	-30	-10	-2	7	20	50
	-110	-100	-80	-75	-45	-30	-10	-2	15	20	50
	-110	-100	-80	-75	-52	-25	-10	-2	3	20	50
	-110	-100	-80	-75	-52	-25	-10	-2	2	20	50
	-110	-100	-80	-75	-52	-25	-10	-2	2	20	50
	-110	-100	-80	-75	-52	-25	-10	-2	2	15	50
Verical Coordinate	90	90	90	90	90	90	90	90	90	90	90
	80	80	80	80	80	80	80	80	80	80	80
	70	70	70	70	70	70	70	70	70	70	70
	65	65	65	65	65	65	65	65	65	65	65
	45	45	45	45	45	35	29	27	35	35	35
	37	37	37	37	32	25	22	6	10	10	10
	10	10	10	10	10	10	7	5.5	5.5	5.5	5.5
	5	5	5	5	5	5	2	2	2.5	2.5	2.5
	0	0	0	0	0	0	0	0	0	0	0
Mesh Sections	IN Z FROM	TO	IN R FROM	TO	TYPE OF MATERIAL						
	2	5	2	65	1						
	5	82	2	5	1						
	72	82	5	7	1						
	72	82	7	25	1						
	72	82	25	35	1						
	72	82	35	55	1						
	72	82	55	65	1						
	5	7	35	65	1						
	7	27	35	65	1						
	27	42	35	65	1						
	42	52	35	65	1						
	52	62	35	65	1						
	7	27	7	25	3						
	42	62	7	25	3						
Current Density	1										
Magnetization	0	0									
	0	0	0	0							
	0	0	0	0							

FIG. 2. Sample data preparation for FEM-CMFD program.

Magnetic Field Calculations of Typical Magnetic Lens:

To test the performance and the accuracy of the new program (FEM-CMFD), the asymmetrical lens designed by Al-Khaldey [47] (shown in Figs. 3 and 4) was used for both analytical and practical testing.

The fine and coarse mesh distributions of the Finite Element Method (FEM) and the geometry border determinations for the tested lens are organized as illustrated in Fig. 4. Subsequently, the input data file for the FEM-CMFD program is prepared in a manner previously shown in Fig. 2.

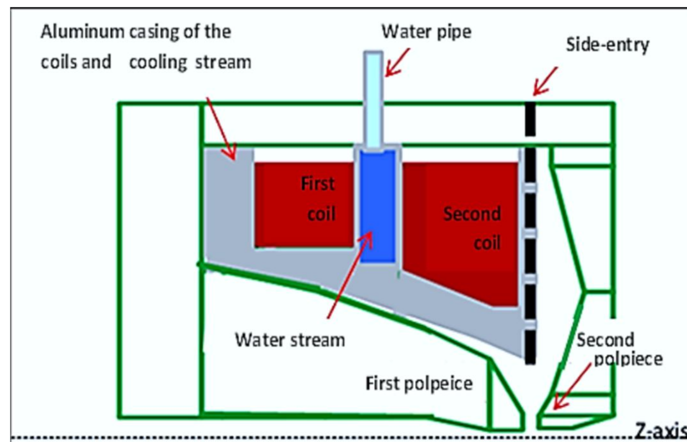

FIG. 3. Cross-section of half of the asymmetrical magnetic lens introduced by Al-Khaldey [47] which is used for analytical and practical tests of the FEM-CMFD program.

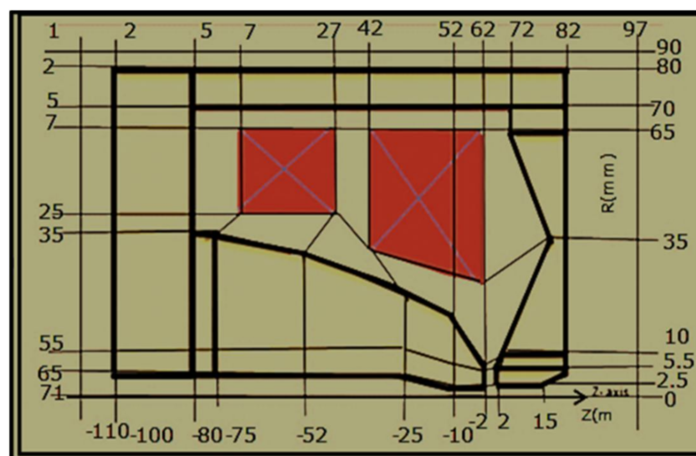

FIG. 4. The FEM's fine and coarse mesh distributions of the tested lens introduced by Al-Khaldey [47].

With the aid of the FEM-CMFD program, the output axial magnetic field distribution data can be either edited or directly plotted. Fig. 5 shows the field distribution of the axial magnetic field for the tested lens. This representation has been generated by the program using the Graph button and has been calculated at an excitation of 2000 A-t.

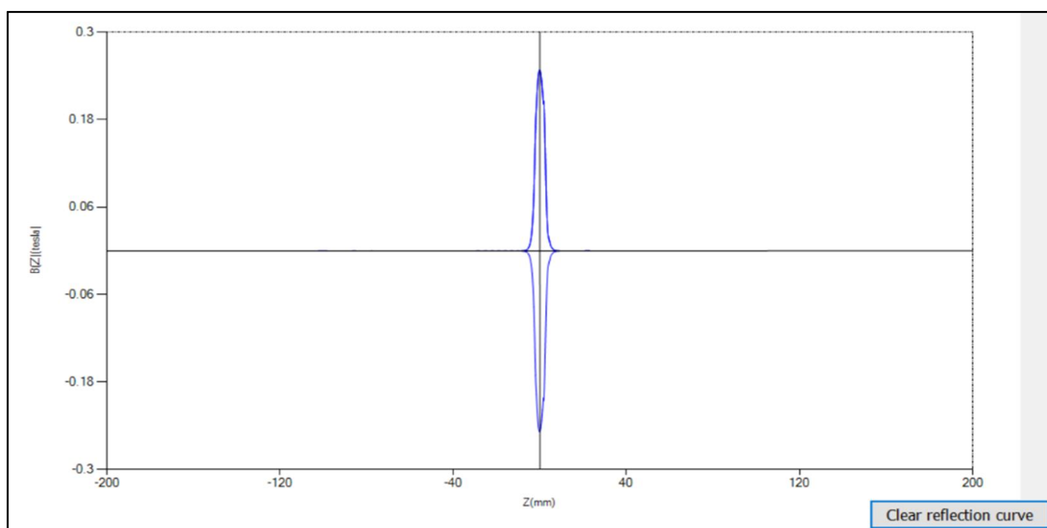

FIG. 5. The axial magnetic field distribution of the tested lens as demonstrated by the program FEM-CMFD, which is calculated at an excitation of 2000 A-t.

In addition, the FEM-CMFD program can export field data to Microsoft Excel, enhancing the representation of data. Figure 6 shows the magnetic field of the tested lens designed by Al-Khaldey, calculated using the FEM-CMFD program at excitations of 1, 2, 3, 4, 5, 7, 10, 20, 50, and 100 kA-t. Notably, at excitation values of 20, 50, and 100 kA-t, saturation effects become evident in the field profile. These effects arise from the magnetic field straying from the iron circuit of the lens.

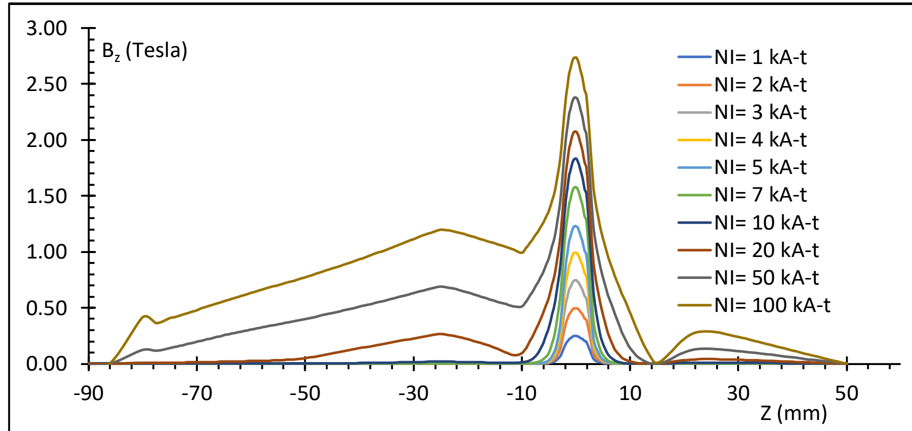

FIG. 6. The magnetic field of the tested lens of Al-Khaldey [47] calculated using the FEM-CMFD program at excitations of 1, 2, 3, 4, 5, 7, 10, 20, 50, and 100 kA-t.

The variations of the maximum field value with the lens excitations are illustrated in Fig. 7. The curves in this figure closely resemble the magnetization curves of soft iron. This match serves as confirmation of the validity of the new program.

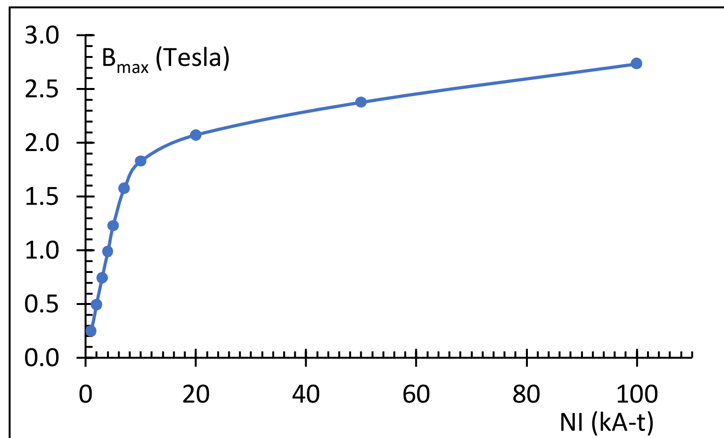

FIG. 7. The variation of the maximum value of the field with the lens excitations.

Furthermore, an additional comparison for the magnetic field calculations has been conducted with another magnetic lens (shown in Fig. 8), introduced by Zlámal and Lencová [48, 49]. The computations were performed using both the EOD program [50] and the FEM-CMFD program to determine the magnetic field at a constant excitation of NI=500 A-t. Figure 9 illustrates a comparison between the axial magnetic field profile, showcasing a perfect agreement between the two curves, considering the errors inherent in numerical calculations.

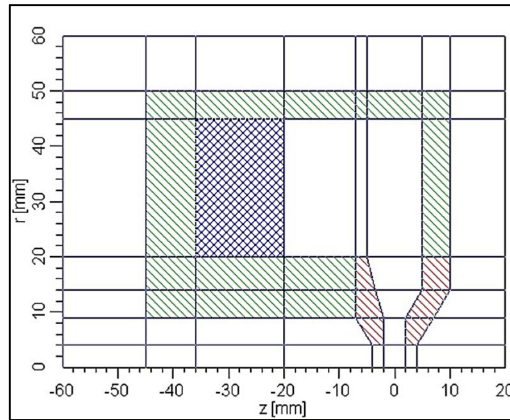

FIG. 8. Cross-section of one-half of the asymmetrical magnetic lens introduced by Zlámal & Lencová [48, 49], which is used for testing the new program (FEM-CMFD).

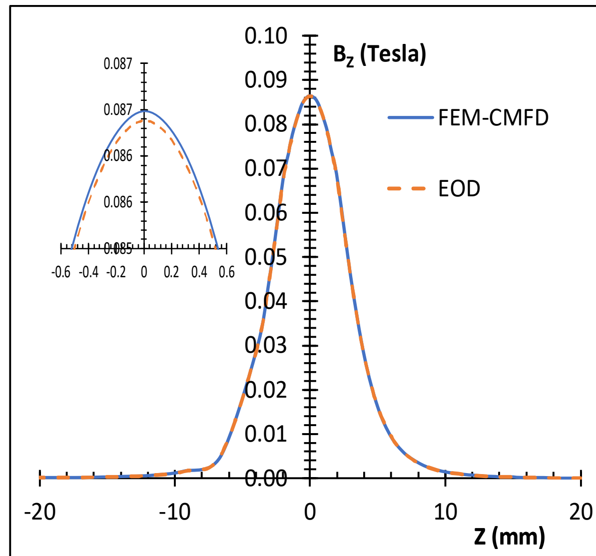

FIG. 9. Comparison between the axial magnetic field due to the second test lens, calculated at NI=500 A-t using EOD and FEM-CMFD programs.

The present program is equipped with an automatic correction feature to address accepted error values set at 10^{-12}. In cases where the numerically calculated area value under the field curve deviates from the input excitation value, the program initiates a recalculation with the addition of a correction factor. This process continues iteratively until the required accuracy is achieved, following Maxwell's fourth equation. Seven allowed approximations are granted, providing the program the opportunity to reach the required accuracy. If, after these attempts, the program cannot attain the specified accuracy (when comparing the input excitation and the area under the curve), it will halt, prompting the operator to redesign the meshes in the FEM calculations. Errors in programs calculating magnetic fields in magnetic lenses using FEM often stem from inappropriate mesh distribution for a specific design. In such cases, the program ceases operation and notifies the operator to reevaluate the mesh distribution. The error tolerance in our program is set at $\epsilon = 10^{-12}$. This comprehensive error-handling mechanism ensures the reliability and precision of the calculations, promoting accurate results in the magnetic field simulations.

Conclusions:

The present work introduces a new program for the calculation of the axial magnetic field of rotationally symmetric magnetic lenses. Referred to as "FEM-CMFD," which stands for "Finite Element Method for Calculating Magnetic Field Distribution", this program underwent testing by comparing its results with those of previously published research works. The comparison revealed a perfect agreement, accounting for errors inherent in numerical computations associated with different methods.

References:

[1] Park, M.-J., Kim, D.H., Park, K., Jang, D.Y. and Han, D.-Ch., J. Mech. Sci. Technol., 22 (2008) 1734.

[2] Bogner, A., Jouneau, P.-H., Thollet, G., Basset, D. and Gauthier, C., Micron, 38 (2007) 390.

[3] Al-Azawy, A.A.R., Al-Kadumi, A.K.S. and Najm, Z.N., J. Kerbala University, 15 (1) (2017) 186.

[4] Paris, G.Y., Nucl. Instrum. Methods, 44 (1) (1966) 137.

[5] Kasper, E., "Magnetic Field Calculation and Determination of the Electron Trajectories", Magnetic Electron Lenses, Ed. W. Hawkes, (Berlin, Springer, 1982) pp 57 – 118.

[6] Lencovà B., "CAD in Electron Optics", Report, Institute of Scientific Instruments of the ASCR, Královopolsk 147, Brno, Czech Republic, (2007).

[7] Lencovà B., "Software for Particle Optics Computations SPOC", Fleischnerova 15, 63500 Brno, Czech Republic, (2000).

[8] Fujita, Sh., Takebe, M. and Shimoyama, H., G-Optk, 7th International Conference on Charged Particle Optics (CPO-7), Abstract for Computer Software Demonstrations, Trinity College Junior, Parlour, (2006).

[9] Lencovà B. and Zlámal J., Microsc. Microanal., 13 (3) (2007) 2.

[10] Müller, H., Uhlemann, S., Hartel, P. and Haider, M., Proceeding of CPO-7, Eds. E. Munro and J. Rose, Physics Procedia, Vol. 1No. 1, (2008) pp. 167-178.

[11] Trubitsyn, A.A., Appl. Phys. (Rus.), 2 (2008) 56.

[12] Dahl, D.A., Int. J. Mass Spectrom., 200 (2000) 3.

[13] Manura, D., "SIMION ® 8.0 User Manual", (Scientific Instrument Service (SIS), Inc., issue 172, USA, 2008).

[14] Huang, T., Hu, Q., Yang, Z., Li, B., Li, J.Q., Jin, X.L., Hu, Y.L., Zhu, X.F., Liao, L., Xiao, L. and He, G.X., Electron Devices, IEEE Transactions, 56 (1) (2009) 140.

[15] Munro, E., "Munro's Electron Beam Software – Software Catalogue", (MEBS Ltd, 2010).

[16] Humphries, S., "Three-Dimensional Charged-particle Optics and Gun Design", (Field Precision LLC, CRC Press, Albuquerque, New Mexico U.S.A, 2011).

[17] Egerton, R.F., "Physical Principles of Electron Microscopy", (Springer, USA, 2005).

[18] Szilagyi, M., "Electron and Ion Optics", (Plenum Press: New York, 1988).

[19] Hawkes, P.W., "Magnetic Electron Lenses", (Springer-Verlag, Berlin, 1982).

[20] Liebl, H., "Applied Charged Particle Optics", Ch.1-4, (Springer, 2008) pp. 1-104.

[21] Hasan, H.S., Int. Lett. Chem. Phys.Astron., 4 (2013) 46.

[22] Arabi, E., Arabi, A., KamaliI, S.M., Horie Y., and Farpon, A., Optica, 3 (6) (2016) 628.

[23] Al-Obaidi, H.N. and Al-Azawy, A.A.R., J. Coll. Educ., 1 (2016) 39.

[24] Ghani, M.K.A., Mohammed, M.A., Ibrahim, M.S., Mostafa, S.A. and Ibrahim, D.A., J. Theor. Appl. Inf. Technol., 95 (13) (2017) 3127.

[25] Ogudo, K.A., Nestor, M.J.D., Khalaf, O.I. and Kasmaei, D.H., IOT Services and Machine-Type Communication in Cellular Networks Symmetry, 11 (2019) 593.

[26] Mohammed, M.A., Ghani, M.K.A., Mostafa, S.A. and Ibrahim, D.A., J. Eng. Appl. Sci., 12 (2017) 4792.

[27] Kadim, W.J., Naser, B.A. and Abbas, T.M., Int. J. Eng. Technol., 7 (4) (2018) 3591.

[28] Khalaf, O.I, Abdulsahib, G.M. and Sadik, M., J. Eng. Appl. Sci., 13 (2018) 9277.

[29] Khalaf, O.I. and Sabbar, B.M., Period. Eng. Nat. Sci., 7 (3) (2019) 1096.

[30] Alabdullah, A.I.M., Mostafa, S.A., Mohammed, M.A., Mustapha, A., Ramli, A.A., Jubair, M.A., Hassan, M.H., Ismail, A. and Ibrahim, D.A., Revista Aus., 26 (1) (2019) 199.

[31] Alabdullah, A.I.M. Ph.D. Thesis, Mosul University, Mosul, Iraq, (2013).

[32] Tahir, K. and Mulvey, T., Inst. Phys. Conf. Ser., 119 (12) (1991) 211.

[33] Munro, E., "Some Technique and Applications of the Finite Element Method for Solving Magnetic Field Problems", Proc., (1976).

[34] Lencova', B., "On the use of finite element method for the computation of electron optical elements", Inst. of Sci. Instru. Czech Academy of Sci., 147, 61264 Brno, Czechoslovakia, (1986a) pp.813-819.

[35] Lencova', B. and Wisselink, G., Nucl. Instr. Meth. in Phys. Res. A, 298 (1-3) (1990) 56.

[36] Podbrdsky, S. and Krivanek, O.L., J. Optik, 79 (1988) 177.

[37] Hill, R. and Smith, K.C.A., Inst. Phys. Conf. Ser., 52 (1) (1980) 49.

[38] Hawkes, P.W. and Kasper, E., "Principles of Electron Optics". Part 2, (Academic Press, London, Ch.44, 1989) pp. 918 – 933.

[39] Munro, E., "Computer- Aided Design of Electron Lenses by the Finite Element Method", In "Image Processing and Computer Aided Design in Electron Optics" Ed. P.W. Hawkes, (Academic Press, London, 1973) pp. 284- 323.

[40] Lencova', B., "The impact of electron optical simulations on the design in electron microscopy", ICEM 13-PARIS, (Optics and detection of charged particles, 1994) pp. 145-148.

[41] Lencova', B., Proc. Conf. Elect. Microscopy, Slovakia (1995) pp.19-23.

[42] Orloff, J., "Handbook of Charged Particle Optics", QC372.2.D4H36, (Library of Congress Cataloging-in-Publication Data, Computational Techniques for Design of Charged Particle Systems, 1997) pp. 13-17.

[43] Glaser, W., Magazine for Physics, 80 (1933) 451.

[44] Scherzer, O., Magazine for Physics, 101 (1936) 593.

[45] Grivet, P., "Electron Optics", 2nd English Ed., Part 1, (Pergamon, Oxford, 1972) pp. 168-170.

[46] Munro, E., "A Set of Computer Programs for Calculating the Properties of Electron Lenses", Report, Cambridge University, Eng. Dept., CUED/B-ELECT/TR 45, (1975).

[47] Al-Khaldey, T.J., Ph.D. Thesis, University of Mosul, Iraq, (2017).

[48] http://www.lencova.com/

[49] Zlámal, J. and Lencová, B., Nucl. Instrum. Meth. A, 645 (1) (2011) 278.

[50] Lencová, B. and Zlámal, J., Physics Proc, 1 (1) (2008) 315.